Molecular Immunology xxx (2009) xxx–xxx

Contents lists available at ScienceDirect

Molecular Immunology

journal homepage: www.elsevier.com/locate/molimm

Light chain somatic mutations change thermodynamics of binding and water coordination in the HyHEL-10 family of antibodies

Mauro Acchione[a], Claudia A. Lipschultz[a], Morgan E. DeSantis[a,1], Aranganathan Shanmuganathan[a], Mi Li[b,c], Alexander Wlodawer[b], Sergey Tarasov[d], Sandra J. Smith-Gill[a,*]

[a] Structural Biophysics Laboratory, Center for Cancer Research, National Cancer Institute, Frederick, MD, USA
[b] Macromolecular Crystallography Laboratory, Center for Cancer Research, National Cancer Institute, Frederick, MD, USA
[c] Basic Research Program, SAIC-Frederick, Frederick, MD, USA
[d] Biophysics Resource in the Structural Biophysics Laboratory, Frederick, MD, USA

ARTICLE INFO

Article history:
Received 14 August 2009
Accepted 28 August 2009
Available online xxx

Keywords:
Enthalpy
Van't Hoff
Affinity maturation
CDR
Flexibility
Glycine
Water
X-ray crystallography

ABSTRACT

Thermodynamic and structural studies addressed the increased affinity due to L-chain somatic mutations in the HyHEL-10 family of affinity matured IgG antibodies, using ITC, SPR with van't Hoff analysis, and X-ray crystallography. When compared to the parental antibody H26L26, the H26L10 and H26L8 chimeras binding to lysozyme showed an increase in favorable ΔG° of -1.2 ± 0.1 kcal mol^{-1} and -1.3 ± 0.1 kcal mol^{-1}, respectively. Increase in affinity of the H26L10 chimera was due to a net increase in favorable enthalpy change with little difference in change in entropy compared to H26L26. The H26L8 chimera exhibited the greatest increase in favorable enthalpy but also showed an increase in unfavorable entropy change, with the result being that the affinities of both chimeras were essentially equivalent. Site-directed L-chain mutants identified the shared somatic mutation S30G as the dominant contributor to increasing affinity to lysozyme. This mutation was not influenced by H-chain somatic mutations. Residue 30L is at the periphery of the binding interface and S30G effects an increase in hydrophobicity and decrease in H-bonding ability and size, but does not make any new energetically important antigen contacts. A new 1.2-Å structure of the H10L10–HEL complex showed changes in the pattern of both inter- and intra-molecular water bridging with no other significant structural alterations near the binding interface compared to the H26L26–HEL complex. These results highlight the necessity for investigating both the structure and the thermodynamics associated with introduced mutations, in order to better assess and understand their impact on binding. Furthermore, it provides an important example of how backbone flexibility and water-bridging may favorably influence the thermodynamics of an antibody–antigen interaction.

Somatic mutation of B-cell receptors, followed by clonal selection and expansion, is an essential vertebrate immune mechanism for developing highly specific and potent antibody response. Somatic mutations occur throughout the H- and L-chains. Mutations in the binding loops making up the complementarity determining regions (CDR) and in the supporting framework regions (FR) can have an important influence on binding affinity and specificity (Thielges et al., 2008; Torres and Casadevall, 2008; Weitkamp et al., 2005). Identification and thermodynamic characterization of somatic mutations which increase affinity and/or change specificity often provide important details on strategies that can be applied to other protein interactions (Chowdhury and Pastan, 1999; Dougan et al., 1998; Du et al., 2007; Kumagai et al., 2003; Lavoie et al., 1992; Sagawa et al., 2003; Thielges et al., 2008). This has direct relevance, but is not limited to, the strong interest in the therapeutic use of antibodies (Jain et al., 2007; Presta, 2006; Yan et al., 2008).

Identifying energetically favorable somatic mutations from sequence data or X-ray structures of complexes is a difficult challenge (Dixon et al., 2002; Welfle et al., 2003). The structure of an antibody–antigen complex can identify non-bonded contacts, hydrogen bonds, salt bridges and localization of hydrophobic and hydrophilic residues that are potentially important to binding to the antigen. The effects of mutations or their relative importance can still be very difficult to predict or interpret from structures

Abbreviations: CDR, complementary determining region; HEL, hen egg white lysozyme; SPR, surface plasmon resonance; ITC, isothermal titration calorimetry; FR, framework residues; RU, response unit; IgG, immunoglobin G; SASA, solvent accessible surface area.

* Corresponding author. Tel.: +1 301 846 5203; fax: +1 301 846 6326.
E-mail address: SmithGiS@mail.nih.gov (S.J. Smith-Gill).
[1] Current address: Department of Biochemistry and Biophysics, University of Pennsylvania, Philadelphia, PA, USA.

0161-5890/$ – see front matter © 2009 Published by Elsevier Ltd.
doi:10.1016/j.molimm.2009.08.018

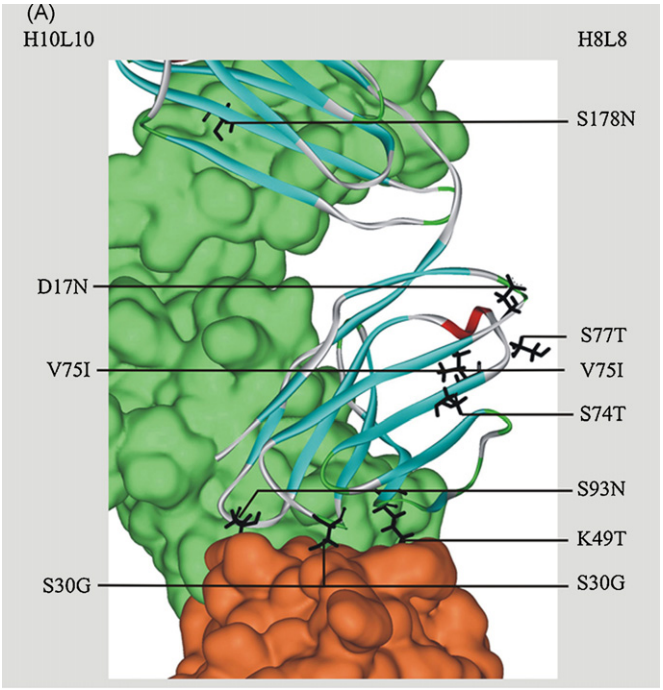

(B)

Position	17	30	49	74	75	77	93	178
H26L26	D	S	K	S	V	S	S	S
H26L10	N	G	K	S	I	S	S	S
H26L8		G	T	T	I	T	N	N

Fig. 1. (A) Spatial relationship of somatic mutations in the structure of H26L26 in complex with HEL (PDB ID: 1NDM). H-chain (green) and lysozyme (orange) are displayed as van der Waals surfaces. The L-chain backbone is modeled in ribbon form. Somatic mutations are highlighted in stick form (black). (B) Sequence summary of amino acid changes resulting from somatic mutation compared with H26L26 (For interpretation of the references to color in this figure legend, the reader is referred to the web version of the article).

alone. Thermodynamic characterization is essential for the unambiguous identification of those residues that provide favorable energetic contributions to antigen binding.

Three independently derived affinity matured IgG antibodies (HyHEL-26, HyHEL-10, and HyHEL-8) recognize similar coincident epitopes on the antigen HEL. All use the same V_L germline gene (Igk-V23) with identical V–J junctions. The only differences between the L-chain sequences are from somatic mutations (Fig. 1) (Lavoie et al., 1999). HyHEL-26 is the least evolved (early secondary), lowest affinity, and least cross reactive in this family. Both HyHEL-10 and HyHEL-8 are late secondary hyper-immune IgGs and exhibit higher affinity and greater cross reactivity with HEL mutants. Together, these three antibodies represent a useful model of an *in vivo* engineering response for improving affinity for a protein antigen.

Many H-chain somatic mutations in these affinity-matured antibodies have been characterized (Newman et al., 1992; Shiroishi et al., 2007; Smith-Gill et al., 1984, 1982), but much less is known about the L-chain somatic mutations. Here we identify functionally significant L-chain residues and detail their structural impact relative to two-step thermodynamic analysis using a new 1.2 Å structure of the HyHEL10 Fab–HEL complex. The impact of heavy chain context is also explored. A single serine to glycine substitution in CDR1 at the periphery of the binding interface significantly increases affinity and alters the binding thermodynamics but does not result in large perturbations in the structure of the complex.

1. Materials and methods

1.1. Protein expression, refolding and purification

Hen egg white lysozyme (Worthington Biochemicals, NJ, USA) was further purified using gel filtration chromatography. The isolation of IgGs and construction of the corresponding recombinant Fab fragment expression system have been described elsewhere (Lavoie et al., 1992; Newman et al., 1992). Fab L- and H-chains were expressed separately in BL21(DE3) (EMD Biosciences, San Diego, CA) cells as inclusion bodies at 37 °C. Expression, isolation and purification of inclusion body protein followed previously outlined procedures (Li et al., 2003). Refolded protein was concentrated 20-fold, buffer exchanged (10 mM Tris, 2 mM EDTA, pH 8.0) using a TTF filter (Pall Corp, East Hills, NY), and loaded onto a DEAE Sepharose Fast-flow column (GE Healthcare Bio-Sciences, Uppsala, Sweden). Sample was eluted with a linear gradient (0–400 mM NaCl over 3 column volumes). Soluble Fab was the first protein to elute and corresponding fractions were pooled, concentrated, and further purified using a Superdex 75 HR gel filtration column (GE Healthcare Bio-Sciences, Uppsala, Sweden). Purity of samples was assessed using SDS-PAGE and elution profiles from gel filtration. For all subsequent analysis, samples were extensively dialyzed against HBS buffer (10 mM HEPES, 150 mM NaCl, 2 mM EDTA, pH 7.4). Fabs of wild type H26L26, and chimeric H26L10 and H26L8 were successfully refolded from bacterial inclusion bodies as judged by the ability to selectively bind HEL using SPR. Contamination from misfolded soluble aggregates and chain homodimers was eliminated using ion exchange and gel filtration chromatography. An unstable off-pathway intermediate from the refolding process formed a soluble metastable aggregate that bound more strongly to the ion exchange column than the properly folded Fab. This species bound to the antigen lysozyme in SPR assays, albeit with much reduced affinity (data not shown), precluding use of an HEL-affinity column for purification purposes. This species was eliminated in the void volume of the gel filtration column. Total yield from the refolding process, measured as the amount of soluble, properly folded protein, ranged from 5 to 45% of the starting material. Stock protein samples were stored at 4 °C in HBS buffer in the presence 0.02% sodium azide until further use. Stability of samples under these storage conditions was evaluated after six months and there was no degradation, aggregation or change in kinetics as judged by gel filtration chromatography and SPR (data not shown).

1.2. Site-directed mutagenesis

Sequence changes to the H26L26 L-chain corresponding to the naturally occurring somatic mutations were introduced individually using the Quikchange II Mutagenesis kit (GE Healthcare Bio-Sciences, Uppsala, Sweden). All mutations were verified by sequencing (DNA Sequencing Laboratory NCI-Frederick, MD, USA).

1.3. Isothermal titration calorimetry

All purified protein samples were prepared for ITC analysis by co-dialyzing extensively against HBS. Measurements were made using a VP-ITC Microcalorimeter (MicroCal LLC, MA, USA) at 15, 25 and 35 °C. Experiments consisted of injections of 8 μL aliquots of 0.10–0.25 mM HEL into 10–25 μM Fab in the ITC cell. This was preceded by a single initial 3 μL injection to minimize impact of diffusion at the ligand/protein interface of the syringe tip during thermal equilibration. Experiments were repeated using dialysis buffer to replace the antibody in the cell. These 'blank' measurements were subtracted from the ligand-into-Fab titration results.

The integrated interaction heat values were fitted to the one-binding site model using Microcal Origin software, yielding the

Please cite this article in press as: Acchione, M., et al., Light chain somatic mutations change thermodynamics of binding and water coordination in the HyHEL-10 family of antibodies. Mol. Immunol. (2009), doi:10.1016/j.molimm.2009.08.018

binding affinity K_A, stoichiometry, standard enthalpy ΔH° and entropy ΔS°. For evaluation of the change in heat capacity ΔC_p°, the change in ΔH was plotted against temperature and fit using a linear least squares model.

1.4. Surface plasmon resonance

Pre-equilibrium rate constants for binding were determined using a Biacore 2000 (GE Healthcare Bio-Sciences, Uppsala, Sweden) instrument. Stock antibody samples were diluted in Biacore HBS buffer (GE Healthcare Bio-Sciences, Uppsala, Sweden) and passed over a CM5-dextran chip immobilized with different levels of amine-coupled HEL ranging from 60 response units (RUs) to 150 RUs. Previous work has shown that the interaction of these antibodies with HEL results in complex two-step binding kinetics that are best evaluated using a series of different injection times (Lipschultz et al., 2000; Wilson et al., 1996) (see Supplementary Material for further explanation of the model),

$$A + B \underset{k_{-1}}{\overset{k_1}{\rightleftarrows}} AB^1 \underset{k_{-2}}{\overset{k_2}{\rightleftarrows}} AB^2 \quad (1)$$

A and B represent the antibody and antigen respectively, AB^1 is Complex I and AB^2 represents Complex II, which has undergone a conformational rearrangement from Complex I to a more stable form. The SPR experimental protocol consisted of four analyte-inject (association) times of 10 min, 25 min, 60 min and 120 min, followed by a 2-h dissociation period with HBS buffer. Blank flow cell corrected sensorgrams were then pooled for global fitting using the two-step model (Eq. (1)). Van't Hoff analysis of the binding constants at six different temperatures was used to determine $\Delta H^{\circ(SPR)}$. Error analysis of van't Hoff data used standard errors reported for the regression. Replicates data points at each temperature were included in the regression (see Supplementary Material). The $\Delta G^{\circ(SPR)}$ and $\Delta S^{\circ(SPR)}$ were calculated using standard thermodynamic relationships,

$$\Delta G^\circ = -RT \ln K_A \quad (2)$$

$$\Delta G^\circ = \Delta H^\circ - T\Delta S^\circ \quad (3)$$

1.5. Crystallization, data collection, and structural determination of the HyHEL-10 Fab–HEL complex

Crystals of HyHEL-10 Fab (7.2 mg/mL) in a 1:1 molar complex with HEL were grown in a hanging drop by vapor diffusion in 0.2 M di-ammonium citrate, 20% PEG 3350, pH 7.0, at room temperature over seven days. Diffraction data were collected on these crystals at the Argonne National Laboratories Advanced Photon Source, at SER-CAT, BM-22 (Argonne, IL, USA) and processed using HKL2000 (Otwinowski and Minor, 1997). The structure was solved by molecular replacement using Phaser (McCoy et al., 2007) using the coordinates 1NDM as a starting model and refined with REFMAC5 (Murshudov et al., 1997). A summary of data collection and refinement parameters, as well as evaluation of the structure, is presented in Table 2.

2. Results and discussion

2.1. Net binding thermodynamics

As monitored by ITC, the binding of parental H26L26[2] and two chimeras (H26L10 and H26L8) to HEL exhibited sharp transitions

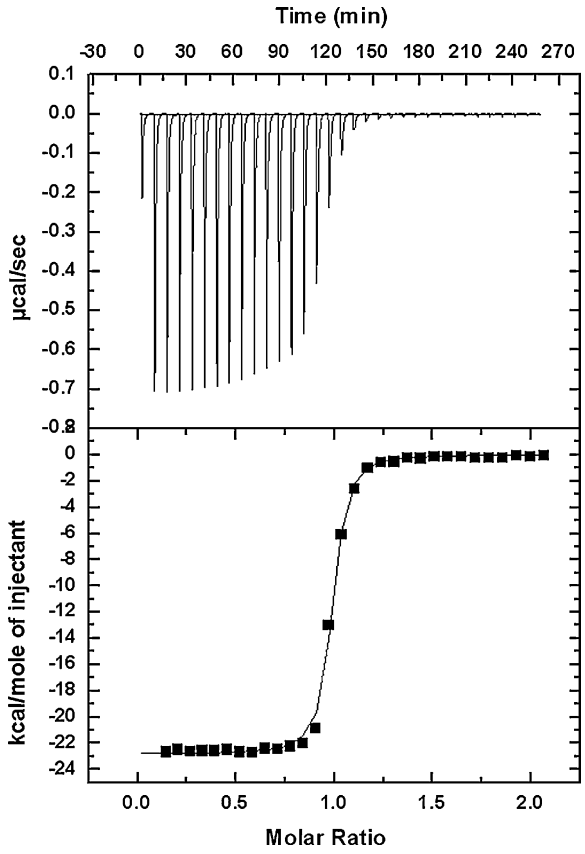

Fig. 2. ITC experiment with H26L10 binding to HEL. The binding isotherm (above) was integrated to give the change in enthalpy plotted as a function the molar ratio of HEL:Fab (below). The point of transition during titration confirms a 1:1 molar binding ratio of Fab to HEL.

(precluding an accurate estimation from ITC of K_A which is in the mid to low nanomolar range) at 1:1 (antibody:antigen) molar ratios during the titration. This stoichiometry confirmed the expected single binding site and sample homogeneity (Fig. 2). Values for ΔG° were estimated from SPR binding data. Chain chimeras formed much more stable complexes than parental H26L26 (Table 1). Both chain chimeras gained essentially equivalent favorable ΔG°, but with differing underlying thermodynamics.

All three complexes exhibited large favorable changes in $\Delta H^{\circ(ITC)}$ and $\Delta H^{\circ(SPR)}$ (obtained by linear van't Hoff analysis of SPR binding at different temperatures) (Fig. 3; Table 1). Both chimeras derived a greater ΔH° than H26L26 as measured by both methods. The $\Delta H^{\circ(SPR)}$ estimate for H26L8 was very similar to $\Delta H^{\circ(ITC)}$. However, SPR underestimated the values of $\Delta H^{\circ(SPR)}$ for both H26L10 and H26L26 when compared with ITC. The differences comparing these two methods however are much smaller than what has often been reported in other systems (Liu and Sturtevant, 1995).

Both H26L26 and H26L8 exhibited the same $\Delta C_p^{\circ(ITC)}$ (Fig. 3; Table 1), whereas H26L10 exhibited a decrease in $\Delta C_p^{\circ(ITC)}$ that is different from that of H26L8, but when the higher error associated with the value is taken into account all three antibodies show very similar changes in heat capacity. The $\Delta C_p^{\circ(ITC)}$ values for all these Fab's are very consistent with those observed for the corresponding IgG, with one notable exception being that the change in $\Delta C_p^{\circ(ITC)}$ for H26L8 is significantly lower than that observed for HyHEL-8 IgG

[2] In previous work these antibodies were referenced using the prefix 'HyHEL-' followed by a unique identifying number (ie. HyHEL-26, HyHEL-10, and HyHEL8). In this work we will refer to the refolded Fab using notation that corresponds to the respective H and L-chains in their structure. For example, HyHEL-26 will be referred to here as H26L26 and HyHEL-8 as H8L8, while a chain chimera constructed using the heavy chain from HyHEL-26 and light chain of HyHEL-8 will be referred to as H26L8.

Please cite this article in press as: Acchione, M., et al., Light chain somatic mutations change thermodynamics of binding and water coordination in the HyHEL-10 family of antibodies. Mol. Immunol. (2009), doi:10.1016/j.molimm.2009.08.018

Table 1
Thermodynamic comparison of Fab samples binding to HEL using ITC and SPR van't Hoff analysis. All values are reported with the units kcal mol^{-1} except for ΔC_p°, which is in cal mol^{-1} K^{-1}.

	H26L26	H26L10	H26L8
$\Delta H^{\circ(ITC)}$	−19.9 ± 0.1	−22.8 ± 0.1	−21.6 ± 0.1
$\Delta C_p^{\circ(ITC)}$	−285 ± 3	−253 ± 6	−285 ± 22
$\Delta G^{\circ(SPR)}$	−11.5 ± 0.1	−12.7 ± 0.1	−12.8 ± 0.1
$\Delta H^{\circ(SPR)}$	−17.0 ± 1.3	−18.3 ± 1.9	−21.0 ± 1.0
$-T\Delta S^{\circ(SPR)}$	5.5 ± 1.3	5.6 ± 1.9	8.2 ± 1.2
$\Delta\Delta H^{\circ(SPR-ITC)}$	2.9 ± 1.3	4.6 ± 1.9	0.6 ± 1.0
Complex I			
$\Delta G_1^{\circ(SPR)}$	−10.9 ± 0.1	−11.1 ± 0.1	−10.9 ± 0.1
$\Delta\Delta G_1^{\circ(SPR)}$	NA	0.2 ± 0.1	0.0 ± 0.1
$\Delta H_1^{\circ(SPR)}$	−6.5 ± 2.1	5.1 ± 3.8	3.3 ± 1.1
$\Delta\Delta H_1^{\circ(SPR)}$	NA	11.6 ± 4.3	9.8 ± 2.4
$-T\Delta S_1^{\circ(SPR)}$)	−4.4 ± 2.2	−16.2 ± 3.6	−14.2 ± 1.2
$\Delta\Delta(-T\Delta S_1^{\circ(SPR)})$	NA	−11.8 ± 4.2	−9.8 ± 2.5
Complex II			
$\Delta G_2^{\circ(SPR)}$	−0.6 ± 0.1	−1.6 ± 0.1	−1.9 ± 0.1
$\Delta\Delta G_2^{\circ(SPR)}$	NA	−1.0 ± 0.1	−1.3 ± 0.1
$\Delta H_2^{\circ(SPR)}$	−18.3 ± 2.2	−25.3 ± 3.0	−27.4 ± 1.3
$\Delta\Delta H_2^{\circ(SPR)}$	NA	−7.0 ± 3.7	−9.1 ± 2.6
$-T\Delta S_2^{\circ(SPR)}$)	17.7 ± 2.3	23.7 ± 3.1	25.5 ± 1.4
$\Delta\Delta(-T\Delta S_2^{\circ(SPR)})$	NA	6.0 ± 3.9	7.8 ± 2.7

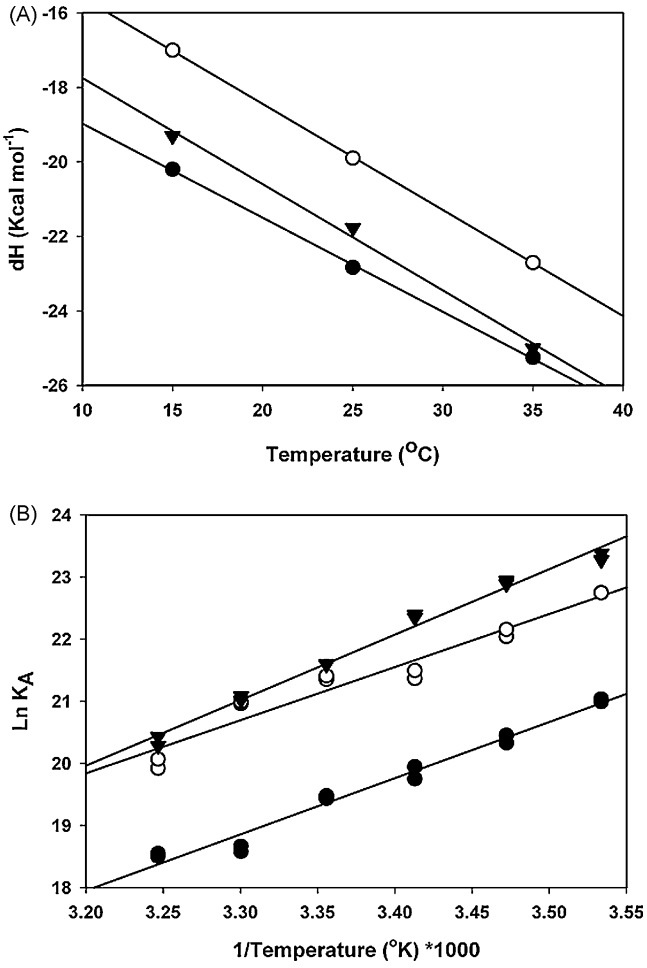

Fig. 3. (A) Determination of the change in ΔC_p° for H26L26 using ITC. ○ H26L26, ● H26L10, ▼ H26L8. B) van't Hoff analysis of SPR binding data. ○ H26L26, ● H26L10, ▼ H26L8. Binding affinity was derived from pre-equilibrium kinetics of association and dissociation using a two-step conformational change binding model.

(Mohan et al., 2009). This was interesting given that the IgG are 3 times larger than the Fab used here and one may have expected a greater difference owing to changes in bulk solvent, bound water or non covalent bonds in the constant regions of IgG. Furthermore, we previously described the importance to binding of H-chain residues and their relative hydrophobicity. The results here indicate that differences in ΔC_p° are solely the result of sequence differences in the H-chain.

2.2. Two-step thermodynamics

This family of antibodies has previously demonstrated two discernable kinetic steps (see Eq. (1) in Section 1). ITC results presented here show that the somatic mutations increased the change in net favorable enthalpy of association, but could not provide details on individual changes occurring in the two-step association. Two-step analysis, over several temperatures, provides complete thermodynamic description for Complex I and the final Complex II (Lipschultz et al., 2000). For all three antibodies, up to 95% of the $\Delta G^{\circ(SPR)}$ of binding occurs during Complex I (Table 1). With H26L26 the changes in entropy and enthalpy are smaller in magnitude when compared with H26L10 and H26L8, but since both components are favorable, the net observed $\Delta G^{\circ(SPR)}$ to form the Complex I is equivalent for all three antibodies, despite differences in overall affinity. However, there are differences in the distribution of enthalpic and entropic components driving this step. H26L26 Complex I is both enthalpically and entropically driven. For the chimeras, Complex I is entirely entropically driven. Thus, in improving the stability of the complex, the S30G mutation has resulted in a shift to increase the importance of energy derived from entropy during the first step.

H26L10 and H26L8 show increases in $\Delta\Delta G_2^{\circ(SPR)}$ in going to the time-dependant Complex II (Copeland et al., 2006; Futamura et al., 2005; Gooljarsingh et al., 2006; Torres et al., 2007) (Table 1). Given that there were no significant differences among the $\Delta\Delta G_1^{\circ(SPR)}$ of the three antibodies, transition to Complex II accounts for the overall greater affinity of the chain chimeras. For each of the three antibodies there is a large favorable change in enthalpy and a significant but smaller change in unfavorable entropy for this step. The magnitudes of $\Delta H_2^{\circ(SPR)}$ and $-T\Delta S_2^{\circ(SPR)}$ were larger than those of the first step for each of the three antibodies despite the observation that $\Delta G_2^{\circ(SPR)}$ was much smaller than $\Delta G_1^{\circ(SPR)}$. The result is a slower dissociation of the final complex. A strategy often observed with high affinity antibodies (Chen et al., 1999), where there are upper limits to increasing the rate of association of the antibody with its antigen when strong ionic interactions are absent (Batista and Neuberger, 1998).

2.3. Residues that increase affinity

Each somatic mutation was introduced individually into the wild type H26L26 L-chain, then expressed and refolded with the H-chain of H26L26. The kinetics for the association at 25 °C was used to compare any changes to $\Delta G^{\circ(SPR)}$ (Fig. 4 black bars). Somatic mutations D17N, K49T, and S74T showed a small unfavorable change to $\Delta G^{\circ(SPR)}$, mutations S93N, S178N V75I, and S77T showed a small favorable change in $\Delta G^{\circ(SPR)}$. None of these mutations accounted for the large difference in binding affinity seen with the chain chimeras. The S30G mutation resulted in a significant increase in binding affinity that closely matched that which was observed with the chain chimeras with a $\Delta\Delta G^{\circ(SPR)}$ of -1.2 ± 0.1 kcal/mol. The increase in affinity observed with the S30G mutation is a result of this increased favorable net enthalpic change in the two chimeras sharing this mutation. Serine is one of the three residues (tyrosine and tryptophan being the other two) that is most often replaced during somatic mutation from germline sequences. Serine mutation most often results in a change to glycine as seen here (Clark

Please cite this article in press as: Acchione, M., et al., Light chain somatic mutations change thermodynamics of binding and water coordination in the HyHEL-10 family of antibodies. Mol. Immunol. (2009), doi:10.1016/j.molimm.2009.08.018

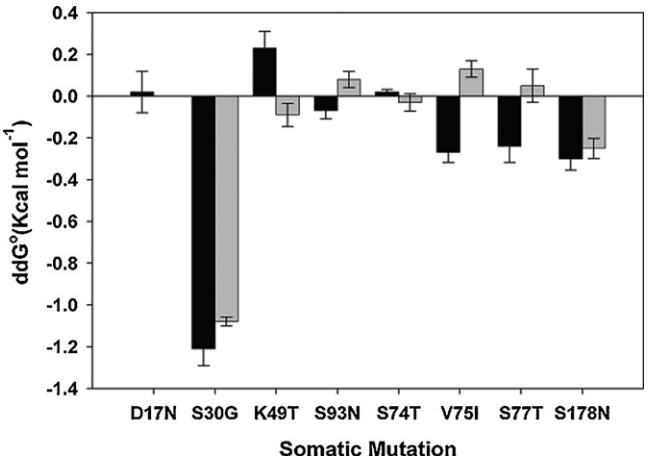

Fig. 4. Summary of the effects on binding affinity with introduction of individual somatic mutations into the L-chains of H26L26 (black) and H8L26 (gray) antibodies.

et al., 2006), thus better understanding the impact on binding in a structural context can have important implications for investigating other antibodies that involve similar substitutions.

2.4. Impact of H-chain origin on L-chain mutants

Similar experiments were conducted using the H-chain of H8L8 (Fig. 4, gray bars) to determine whether concurrent somatic mutations in the H-chain influenced the impact on binding of mutations in the L-chain. The overall affinity of these H8L26 mutants was higher than those of the comparable H26L26 mutants. This reflects the favorable mutations associated with the H8 chain. However, the pattern of changes in $\Delta G^{\circ(SPR)}$ introduced by the corresponding L-chain mutations was very similar between the two groups of antibodies. This indicated that no interaction was occurring with H8 mutations. The $\Delta\Delta G^{\circ(SPR)}$ for the S30G mutation in H8L26 vs. H26L26 was only 0.1 kcal/mol. In addition to S30G, K49T was now slightly favorable to binding, as was S178N. However, S93N, V75I and S77T are now slightly unfavorable. Despite these small differences, the presence of a different H-chain had minimal impact on whether the somatic mutation significantly increased or decreased binding affinity. There was no significant 'cross-talk' between heavy and light chains as far as the light chain mutations are concerned.

2.5. Structural comparisons

Structures for the chain chimeras are not yet available. Our results show that the L-chain somatic mutations do not interact with somatic mutations in the H-chain. We therefore felt confident in using our newly solved high-resolution structure (1.2-Å) of the H10L10 complex to explore any structural differences in and around the region of the S30G mutation. The structure of the H10L10–HEL complex (Table 2) was compared to the available 1.8-Å structure of the H26L26–HEL complex (Li et al., 2003). The C_α backbone overlay of H10L10 and H26L26 shows that the two complexes are very similar with an RMSD of 0.6 Å in the variable (Fv) region (Fig. 5A). The mutation of serine to glycine does not introduce any new energetically significant contacts between L-chain CDR1 and HEL (Fig. 5B). However, two adjacent residues Asn31 and Asn32 do make contacts with epitope hotspots Lys96 and Tyr20 in lysozyme. There are clear differences in size and hydrophobicity of the serine and glycine side chains that may have an influence on this nearby interaction. In comparison to H26L26, the H10L10 SASA goes up from 30.9 to 66.7 at position 30 of the L-chain, however the adjacent residues Asn31 and Asn32 both decrease only slightly by 2.1 and 2.4 respectively. Residue Ser30 is located in the middle of the CDR1 loop at the periphery of the binding interface. This pattern is consistent with the previous observation in the H-chain that also identified important somatic mutations occurring at the periphery of the binding interface (Li et al., 2005; Shiroishi et al., 2007). This mutation may provide a more favorable ensemble of conformations in the free antibody to sample the antigen surface (Bauer and Sticht, 2007; Schramm et al., 2008), accounting for the differences in entropy–enthalpy distribution in forming Complex

Table 2
Crystallographic data and statistics on H10L10–HEL structure.

Space group	*P*21(*P*1211)
Unit cell dimensions	$a = 39.84$ Å, $b = 77.39$ Å, $c = 89.11$ Å; $\alpha = 90^\circ$, $\beta = 96.66^\circ$, $\gamma = 90^\circ$
Resolution (Å)	1.2
R_{merge}	0.039
Completeness (%)	94.3
R-factor	0.191
Free *R*-factor	0.205
Number of reflections (total/unique)	157,734
Amino acid residues	553 (L-210, H-214, HEL-129)[a]
Water molecules	683
Ramachandran plot[b]	
Most favored regions (%)	90.0
Additional allowed regions (%)	9.8
Generously allowed regions (%)	0.0
Disallowed regions (%)	0.2

[a] L: light chain, H: heavy chain, HEL-lysozyme antigen.
[b] Procheck.

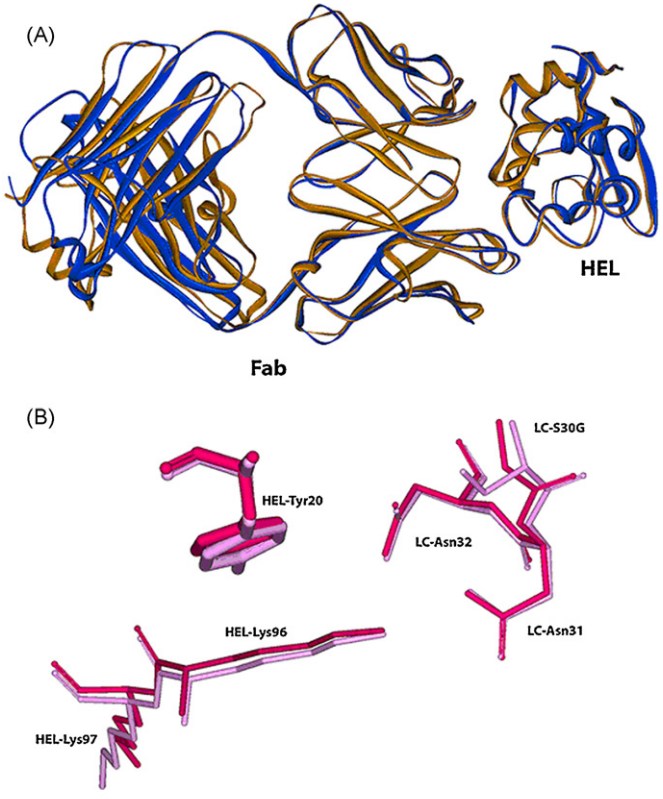

Fig. 5. Comparison of newly solved H10L10–HEL complex (PDB ID: 3D9A) with previously solved H26L26 complex (PDB ID: 1NDM). (A) Ribbon representation of C_α backbone overlay of H10L10 (blue) and H26L26 (orange) complexed with HEL. (B) Close up of superimposed structures (1NDM: pink and 3D9A: red) showing position of the S30G mutation and neighboring Asn31–Asn32 residues relative to HEL hotspots Tyr20 and Lys96 (For interpretation of the references to color in this figure legend, the reader is referred to the web version of the article).

Please cite this article in press as: Acchione, M., et al., Light chain somatic mutations change thermodynamics of binding and water coordination in the HyHEL-10 family of antibodies. Mol. Immunol. (2009), doi:10.1016/j.molimm.2009.08.018

I. Attempts at obtaining crystals of the free H10L10 Fab antibody have so far been unsuccessful, but efforts are continuing.

2.6. Glycine flexibility

Introduction of a glycine may also influence flexibility (Miyazaki et al., 1997; Moiseev et al., 2005) of the CDR1 loop or adjacent residues before or during formation of the complex. The net entropic penalty when forming the complex with H26L8 chimera is greater than for H26L26. With H26L10 the net entropic penalty is similar to that of H26L26. However when we observe the differences during formation of Complex I, there is an increase in favorable entropy for this first step with the chain chimeras bearing the glycine mutation. This comes at the cost of enthalpy. So in gaining the ability to form a more stable Complex II, there is a shift in thermodynamics favoring entropy in forming Complex I. This increase in entropy could certainly be derived from the increase in flexibility that accompanies removing the serine side chain. There are a number of reported examples of how increased flexibility from glycine substitutions can impact protein function. Flexibility of glycine residues is important for substrate binding and release for *E. coli* inorganic pyrophosphatase (Moiseev et al., 2005). In the Lck SH3-domain a proline to glycine substitution increased ligand-binding affinity (Bauer and Sticht, 2007). In the case of enzyme triosephosphate isomerase it was observed that glycine residues were not favorable in the hinge regions of the binding loop (Kempf et al., 2007). The reason cited was a certain degree of rigidification of the loop was necessary for productive movements during catalysis. Introduction of glycine residues in that case would be expected to increase the flexibility of the hinge resulting in non-productive conformers. Antibodies are comparatively naïve protein binders in the context of ever changing antigens to which they must recognize and bind. Even a small change in side chain, such as substitution of alanine for glycine, can destabilize and increase flexibility rather than reduce it (Battiste et al., 2002). This makes predictions of behavior with glycine mutations especially difficult. Also, we have previously reported that affinity maturation of these antibodies reduces salt-links and hydrogen bonds, which reduced rigidity in the antibody–antigen interaction. A substitution from serine to glycine is consistent with those observations. But the question remains how, in the case of the chimeras, the increase in entropy in forming Complex I gives way to a significant entropic penalty in forming Complex II. Conformational flexibility during binding can allow for a productive sampling of various backbone and side chain orientations. Despite this increased flexibility, the final complex may in fact exhibit much lower conformational flexibility at the interface because of close packing and improved van der waal contacts. Further examples, such as the ones presented in this work, are desirable to see if these correlations extend to other systems. An important point here to be made about flexibility of glycine and entropy changes is that glycine would also be expected to increase conformational entropy in the free state. Therefore even if the final complex of H26L26 and the chain chimeras are similar in terms of conformational flexibility, a relative increase in unfavorable entropy would be expected with the glycine substitution if the free antibodies were starting from a point of higher entropy. At this point it is less clear as to why the two chain chimeras show a difference in net entropy–enthalpy change upon binding despite having the same overall change in ΔG°. However, enthalpy–entropy compensation is a common feature observed with mutagenesis experiments.

2.7. Water mediated interactions

An analysis of bridging solvent contacts at the interface of both complexes showed a change in the pattern of water coordination. The H26L26 complex contains two waters at the interface. One water molecule is forming a simple intermolecular bridge to HEL residue Asp18, whereas the other one forms a ternary complex bridging residues 30 and 92 of the L-chain, and also forms a bridge between position 92 of the L-chain and Asp18 in HEL (Fig. 6A). Somatic mutation to Gly30 results in the loss of the serine OH–water hydrogen bond with the result being displacement of one of those water molecules, while the other water has different interacting partners (Fig. 6B). An intramolecular bridge between Gly16 and Asp18 in HEL replaces the antibody intramolecular bridge between Ser30 and Asp92. The intermolecular bridge between Asn92 and Asp18 is maintained in this new ternary complex.

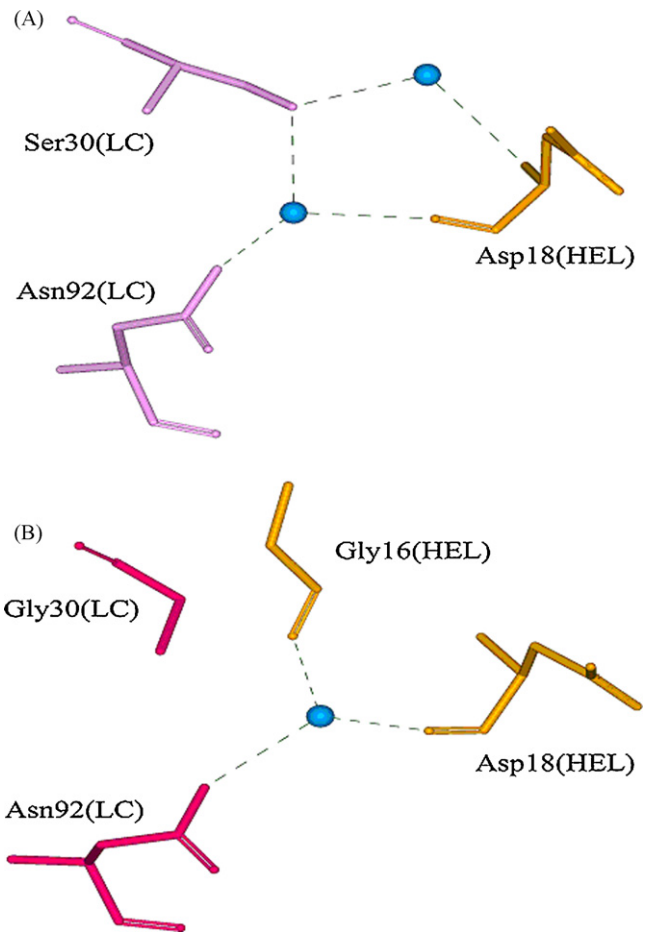

Fig. 6. Change in water pattern at position 30 of the L-chain. (A) H26L26–HEL complex (PDB ID: 1NDM) with the antibody (pink), HEL (orange) and coordinated water (blue). (B) H10L10–HEL complex (PDB ID: 3D9A) with antibody (red), HEL (orange) and coordinated water (blue) (For interpretation of the references to color in this figure legend, the reader is referred to the web version of the article).

Ideally, a comparison of the positions of water molecules between free and complexed forms of the antibody would allow determination of whether these are new waters or whether they are pre-existing in the free antibody or antigen. We have not yet solved structures for free forms of H26L26 or H10L10 Fab. The structures for the family related H63H63 Fab (PDB ID: 1DQM and 1DQQ) are similar in resolution (1.8 and 2.1 Å respectively), with two complexes in the asymmetric unit for 1DQQ. Only one of these complexes shows water coordinated to Asn92 of the L-chain. Having this water coordinated in only one of the structures suggests a transient weak interaction with water at this residue when the antibody is free in solution. The recently solved ultra-high resolution 0.65 Å structure of triclinic HEL (PDB ID: 2VB1) shows that Asp18

Please cite this article in press as: Acchione, M., et al., Light chain somatic mutations change thermodynamics of binding and water coordination in the HyHEL-10 family of antibodies. Mol. Immunol. (2009), doi:10.1016/j.molimm.2009.08.018

coordinates a stable water molecule (Wat2014, 3 hydrogen bonds, low B-factor) in the conformer that is adjacent the Gly16 residue. This water is located on the surface so would not be expected to contribute to fold stability in HEL when free in solution (Reichmann et al., 2008). In S30G complex, one water molecule is apparently lost at the interface and an important bridge between water and the antigen is maintained. This comes from the loss of hydrogen-bonding ability and space occupied by the serine hydroxyl group.

Drawing direct thermodynamic correlations between water accumulation or displacement by a ligand and changes in binding affinity are problematic due to changes in local environment which can dramatically impact the strength of any bridging water molecules (Barillari et al., 2007; Jia et al., 2008). However, the change in hydrogen bond pattern and the difference in water accumulation at the interface in this region would be clearly expected to change the enthalpy–entropy relationship and dynamics for binding. A loss of structured water would be expected to increase favorable entropy upon binding. Furthermore one would have a loss in favorable enthalpy from water hydrogen bonding to protein atoms. Both suggest that loss of bridging water at the interface would have a negative impact on binding. A loss of bridging water can also increase flexibility of the chains that were once bridged. Conformational entropy might be expected to increase under these circumstances. This would be consistent with the increased favorable entropy during formation of Complex I with the chain chimeras. However, bridged chains have a reduced capacity to sample conformation space during binding. This can result in less than optimal positions for protein atoms at the interface, reducing van der waal contacts and preventing optimal hydrogen bond geometry in the final complex. One example highlighting the potential impact of water in a similar system has been reported. A mutation in lysozyme resulted in the uptake of one water at the interface with the antibody HyHEL-5, with a corresponding 1000-fold reduction in affinity (Chacko et al., 1995). Clearly the loss of water at the interface can improve binding, and in our system, the loss of water favors increasing enthalpy and not entropy of association in the final complex. In addition, osmotic pressure experiments showed that changes in water molarity could either increase or decrease binding enthalpy of anti-lysozyme antibodies, which correlated with whether the binding of the respective antibodies was associated with exclusion or maintenance of water molecules bound to the antibody (Braden et al., 1995; Goldbaum et al., 1996). It would be interesting to compare a similar series of antibodies from germline to late-secondary to see if the germline sequence favors entropy over enthalpy when forming the complex.

There is increasing interest in understanding water in modeling and calculating free energies of binding, with the aim of better understanding the role of water in biological interactions (Arcangeli et al., 2008; Fornabaio et al., 2004; Spyrakis et al., 2007). Empirical thermodynamic and structural data, such as those presented here, can help in refining those models by better understanding the changing enthalpy–entropy dynamic during tight binding.

3. Conclusions

Somatic hypermutation during affinity maturation of the HyHEL-10 family of antibodies has produced a S30G L-chain mutation that significantly increases affinity for the antigen and changes water coordination, without significant differences in the peptide backbone or side chain orientation in the complex. This mutation does not interact with somatic mutations in the H-chain. The increase in net affinity reflects increased favorable enthalpy change during formation of the time-dependant final complex (Complex II). Although both H26L10 and H26L8 show essentially the same increase in affinity due to S30G, the 2-step pattern of changes in entropy and enthalpy of binding are different. A new high-resolution structure of HyHEL-10 complex suggests that the glycine residue may influence binding via changes in hydrophobicity or influencing adjacent residues Asn31 and Asn32, as well as altering hydrogen bonding patterns with water molecules at the interface of the S30G mutation, with a net resulting loss of one water molecule. These results support a strategy that uses mutations at the periphery of the binding interface, favoring hydrophobic residues that do not make direct contact with energetically important residues in the target antigen. This model operates by increasing the favorable enthalpy change occurring during formation of Complex II without significant energetic differences in the Complex I, or without any discernable structural change in the structure of the final complex. The exception to this is a change in water pattern at the interface around this mutation. It will be interesting to compare these results with future studies on other antibody–antigen interactions, to determine if there is any correlation with the effects of mutations in regions that perturb pre-existing bound water.

Acknowledgments

Diffraction data were collected at the Southeast Regional Collaborative Access Team (SER-CAT) beamline 22-BM, located at the Advanced Photon Source, Argonne National Laboratory. Use of the Advanced Photon Source was supported by the U.S. Department of Energy, Office of Science, Office of Basic Energy Sciences, under Contract No. W-31-109-Eng-38. We thank Dr. Rob Walter for his assistance in the data collection. This project was supported in part by the Intramural Research Program of the NIH, National Cancer Institute, Center for Cancer Research and in part with Federal funds from the National Cancer Institute, NIH, under Contract No. HHSN261200800001E. The content of this publication does not necessarily reflect the views or policies of the Department of Health and Human Services, nor does the mention of trade names, commercial products, or organizations imply endorsement by the U.S. Government.

Appendix A. Supplementary data

Supplementary data associated with this article can be found, in the online version, at doi:10.1016/j.molimm.2009.08.018.

References

Arcangeli, C., Cantale, C., Galeffi, P., Rosato, V., 2008. Structure and dynamics of the anti-AMCV scFv(F8): effects of selected mutations on the antigen combining site. J. Struct. Biol. 164, 119–133.
Barillari, C., Taylor, J., Viner, R., Essex, J.W., 2007. Classification of water molecules in protein binding sites. J. Am. Chem. Soc. 129, 2577–2587.
Batista, F.D., Neuberger, M.S., 1998. Affinity dependence of the B cell response to antigen: a threshold, a ceiling, and the importance of off-rate. Immunity 8, 751–759.
Battiste, J.L., Li, R., Woodward, C., 2002. A highly destabilizing mutation, G37A, of the bovine pancreatic trypsin inhibitor retains the average native conformation but greatly increases local flexibility. Biochemistry 41, 2237–2245.
Bauer, F., Sticht, H., 2007. A proline to glycine mutation in the Lck SH3-domain affects conformational sampling and increases ligand binding affinity. FEBS Lett. 581, 1555–1560.
Braden, B.C., Fields, B.A., Poljak, R.J., 1995. Conservation of water molecules in an antibody–antigen interaction. J. Mol. Recognit. 8, 317–325.
Chacko, S., Silverton, E., Kam-Morgan, L., Smith-Gill, S., Cohen, G., Davies, D., 1995. Structure of an antibody–lysozyme complex unexpected effect of conservative mutation. J. Mol. Biol. 245, 261–274.
Chen, Y., Wiesmann, C., Fuh, G., Li, B., Christinger, H.W., McKay, P., de Vos, A.M., Lowman, H.B., 1999. Selection and analysis of an optimized anti-VEGF antibody: crystal structure of an affinity-matured Fab in complex with antigen. J. Mol. Biol. 293, 865–881.
Chowdhury, P.S., Pastan, I., 1999. Improving antibody affinity by mimicking somatic hypermutation in vitro. Nat. Biotechnol. 17, 568–572.
Clark, L.A., Ganesan, S., Papp, S., van Vlijmen, H.W., 2006. Trends in antibody sequence changes during the somatic hypermutation process. J. Immunol. 177, 333–340.

Copeland, R.A., Pompliano, D.L., Meek, T.D., 2006. Drug-target residence time and its implications for lead optimization. Nat. Rev. Drug Discov. 5, 730–739.
Dixon, R.W., Radmer, R.J., Kuhn, B., Kollman, P.A., Yang, J., Raposo, C., Wilcox, C.S., Klumb, L.A., Stayton, P.S., Behnke, C., Le Trong, I., Stenkamp, R., 2002. Theoretical and experimental studies of biotin analogues that bind almost as tightly to streptavidin as biotin. J. Org. Chem. 67, 1827–1837.
Dougan, D.A., Malby, R.L., Gruen, L.C., Kortt, A.A., Hudson, P.J., 1998. Effects of substitutions in the binding surface of an antibody on antigen affinity. Protein Eng. 11, 65–74.
Du, J., Wang, H., Zhong, C., Peng, B., Zhang, M., Li, B., Huo, S., Guo, Y., Ding, J., 2007. Structural basis for recognition of CD20 by therapeutic antibody Rituximab. J. Biol. Chem. 282, 15073–15080.
Fornabaio, M., Spyrakis, F., Mozzarelli, A., Cozzini, P., Abraham, D.J., Kellogg, G.E., 2004. Simple, intuitive calculations of free energy of binding for protein-ligand complexes. 3. The free energy contribution of structural water molecules in HIV-1 protease complexes. J. Med. Chem. 47, 4507–4516.
Futamura, M., Dhanasekaran, P., Handa, T., Phillips, M.C., Lund-Katz, S., Saito, H., 2005. Two-step mechanism of binding of apolipoprotein E to heparin: implications for the kinetics of apolipoprotein E-heparan sulfate proteoglycan complex formation on cell surfaces. J. Biol. Chem. 280, 5414–5422.
Goldbaum, F.A., Schwarz, F.P., Eisenstein, E., Cauerhff, A., Mariuzza, R.A., Poljak, R.J., 1996. The effect of water activity on the association constant and the enthalpy of reaction between lysozyme and the specific antibodies D1.3 and D44.1. J. Mol. Recognit. 9, 6–12.
Gooljarsingh, L.T., Fernandes, C., Yan, K., Zhang, H., Grooms, M., Johanson, K., Sinnamon, R.H., Kirkpatrick, R.B., Kerrigan, J., Lewis, T., Arnone, M., King, A.J., Lai, Z., Copeland, R.A., Tummino, P.J., 2006. A biochemical rationale for the anticancer effects of Hsp90 inhibitors: slow, tight binding inhibition by geldanamycin and its analogues. Proc. Natl. Acad. Sci. U.S.A. 103, 7625–7630.
Jain, M., Kamal, N., Batra, S.K., 2007. Engineering antibodies for clinical applications. Trends Biotechnol. 25, 307–316.
Jia, R., Yang, L.J., Yang, S.Y., 2008. Binding energy contributions of the conserved bridging water molecules in CDK2-inhibitor complexes: a combined QM/MM study. Chem. Phys. Lett. 460, 300–305.
Kempf, J.G., Jung, J.Y., Ragain, C., Sampson, N.S., Loria, J.P., 2007. Dynamic requirements for a functional protein hinge. J. Mol. Biol. 368, 131–149.
Kumagai, I., Nishimiya, Y., Kondo, H., Tsumoto, K., 2003. Structural consequences of target epitope-directed functional alteration of an antibody. The case of anti-hen lysozyme antibody, HyHEL-10. J. Biol. Chem. 278, 24929–24936.
Lavoie, T.B., Drohan, W.N., Smith-Gill, S.J., 1992. Experimental analysis by site-directed mutagenesis of somatic mutation effects on affinity and fine specificity in antibodies specific for lysozyme. J. Immunol. 148, 503–513.
Lavoie, T.B., Mohan, S., Lipschultz, C.A., Grivel, J.C., Li, Y., Mainhart, C.R., Kam-Morgan, L.N., Drohan, W.N., Smith-Gill, S.J., 1999. Structural differences among monoclonal antibodies with distinct fine specificities and kinetic properties. Mol. Immunol. 36, 1189–1205.
Li, Y., Li, H., Yang, F., Smith-Gill, S.J., Mariuzza, R.A., 2003. X-ray snapshots of the maturation of an antibody response to a protein antigen. Nat. Struct. Biol. 10, 482–488.
Li, Y., Huang, Y., Swaminathan, C.P., Smith-Gill, S.J., Mariuzza, R.A., 2005. Magnitude of the hydrophobic effect at central versus peripheral sites in protein–protein interfaces. Structure 13, 297–307.
Lipschultz, C.A., Li, Y., Smith-Gill, S., 2000. Experimental design for analysis of complex kinetics using surface plasmon resonance. Methods 20, 310–318.
Liu, Y., Sturtevant, J.M., 1995. Significant discrepancies between van't Hoff and calorimetric enthalpies. II. Protein Sci. 4, 2559–2561.
McCoy, AJ.G.-K.R., Adams, P.D., Winn, M.D., Storoni, L.C., Read, R.J., 2007. Phaser crystallograhic software. J. Appl. Cryst. 40, 658–674.
Miyazaki, S., Shimura, J., Hirose, S., Sanokawa, R., Tsurui, H., Wakiya, M., Sugawara, H., Shirai, T., 1997. Is structural flexibility of antigen-binding loops involved in the affinity maturation of anti-DNA antibodies? Int. Immunol. 9, 771–777.
Mohan, S., Kourentzi, K., Schick, K.A., Uehara, C., Lipschultz, C.A., Acchione, M., Desantis, M.E., Smith-Gill, S.J., Willson, R.C., 2009. Association energetics of cross-reactive and specific antibodies (dagger). Biochemistry.
Moiseev, V.M., Rodina, E.V., Kurilova, S.A., Vorobyeva, N.N., Nazarova, T.I., Avaeva, S.M., 2005. Substitutions of glycine residues Gly100 and Gly147 in conservative loops decrease rates of conformational rearrangements of *Escherichia coli* inorganic pyrophosphatase. Biochemistry (Moscow) 70, 858–866.
Murshudov, G.N., Vagin, A.A., Dodson, E.J., 1997. Refinement of macromolecular structures by the maximum-likelihood method. Acta Crystallogr. D Biol. Crystallogr. 53, 240–255.
Newman, M.A., Mainhart, C.R., Mallett, C.P., Lavoie, T.B., Smith-Gill, S.J., 1992. Patterns of antibody specificity during the BALB/c immune response to hen eggwhite lysozyme. J. Immunol. 149, 3260–3272.
Otwinowski, Z., Minor, W., 1997. Processing of X-ray diffraction data collected in oscillation mode. Macromol. Crystallogr., Pt A 276, 307–326.
Presta, L.G., 2006. Engineering of therapeutic antibodies to minimize immunogenicity and optimize function. Adv. Drug Deliv. Rev. 58, 640–656.
Reichmann, D., Phillip, Y., Carmi, A., Schreiber, G., 2008. On the contribution of water-mediated interactions to protein-complex stability. Biochemistry 47, 1051–1060.
Roos, H., Karlsson, R., Nilshans, H., Persson, A., 1998. Thermodynamic analysis of protein interactions with biosensor technology. J. Mol. Recognit. 11, 204–210.
Sagawa, T., Oda, M., Ishimura, M., Furukawa, K., Azuma, T., 2003. Thermodynamic and kinetic aspects of antibody evolution during the immune response to hapten. Mol. Immunol. 39, 801–808.
Schramm, A.M., Mehra-Chaudhary, R., Furdui, C.M., Beamer, L.J., 2008. Backbone flexibility, conformational change, and catalysis in a phosphohexomutase from *Pseudomonas aeruginosa*. Biochemistry 47, 9154–9162.
Shiroishi, M., Tsumoto, K., Tanaka, Y., Yokota, A., Nakanishi, T., Kondo, H., Kumagai, I., 2007. Structural consequences of mutations in interfacial Tyr residues of a protein antigen–antibody complex. The case of HyHEL-10–HEL. J. Biol. Chem. 282, 6783–6791.
Smith-Gill, S.J., Wilson, A.C., Potter, M., Prager, E.M., Feldmann, R.J., Mainhart, C.R., 1982. Mapping the antigenic epitope for a monoclonal antibody against lysozyme. J. Immunol. 128, 314–322.
Smith-Gill, S.J., Mainhart, C.R., Lavoie, T.B., Rudikoff, S., Potter, M., 1984. VL-VH expression by monoclonal antibodies recognizing avian lysozyme. J. Immunol. 132, 963–967.
Spyrakis, F., Cozzini, P., Bertoli, C., Marabotti, A., Kellogg, G.E., Mozzarelli, A., 2007. Energetics of the protein–DNA–water interaction. BMC Struct. Biol. 7, 4.
Thielges, M.C., Zimmermann, J., Yu, W., Oda, M., Romesberg, F.E., 2008. Exploring the energy landscape of antibody–antigen complexes: protein dynamics, flexibility, and molecular recognition. Biochemistry 47, 7237–7247.
Torres, M., Casadevall, A., 2008. The immunoglobulin constant region contributes to affinity and specificity. Trends Immunol. 29, 91–97.
Torres, M., Fernandez-Fuentes, N., Fiser, A., Casadevall, A., 2007. The immunoglobulin heavy chain constant region affects kinetic and thermodynamic parameters of antibody variable region interactions with antigen. J. Biol. Chem. 282, 13917–13927.
Weitkamp, J.H., Lafleur, B.J., Greenberg, H.B., Crowe Jr., J.E., 2005. Natural evolution of a human virus-specific antibody gene repertoire by somatic hypermutation requires both hotspot-directed and randomly-directed processes. Hum. Immunol. 66, 666–676.
Welfle, K., Misselwitz, R., Hohne, W., Welfle, H., 2003. Interaction of epitope-related and -unrelated peptides with anti-p24 (HIV-1) monoclonal antibody CB4-1 and its Fab fragment. J. Mol. Recognit. 16, 54–62.
Wilson, A.L., Erdman, R.A., Maltese, W.A., 1996. Association of Rab1B with GDP-dissociation inhibitor (GDI) is required for recycling but not initial membrane targeting of the Rab protein. J. Biol. Chem. 271, 10932–10940.
Yan, L., Hsu, K., Beckman, R.A., 2008. Antibody-based therapy for solid tumors. Cancer J. 14, 178–183.

Please cite this article in press as: Acchione, M., et al., Light chain somatic mutations change thermodynamics of binding and water coordination in the HyHEL-10 family of antibodies. Mol. Immunol. (2009), doi:10.1016/j.molimm.2009.08.018